Multiple plume events in the genesis of the peri-Caribbean Cretaceous oceanic plateau province

Henriette Lapierre,[1] Delphine Bosch,[2] Vincent Dupuis,[3] Mireille Polvé,[4] René C. Maury,[5] Jean Hernandez,[6] Patrick Monié,[2] Delphine Yeghicheyan,[4] Etienne Jaillard,[1-7] Marc Tardy,[8] Bernard Mercier de Lépinay,[3] Marc Mamberti,[1-6] Alain Desmet[9], Francine Keller[1], and François Sénebier[1]

Abstract. The oceanic crust fragments exposed in central America, in north-western South America, and in the Caribbean islands have been considered to represent accreted remnants of the Caribbean-Colombian Oceanic Plateau (CCOP). On the basis of trace element and Nd, Sr, and Pb isotopic compositions we infer that cumulate rocks, basalts, and diabases from coastal Ecuador have a different source than the basalts from the Dominican Republic. The latter suite includes the 86 Ma basalts of the Duarte Complex which are light rare earth element (REE) -enriched and display (relative to normal mid-ocean ridge basalts, NMORB) moderate enrichments in large ion lithophile elements, together with high Nb, Ta, Pb, and low Th contents. Moreover, they exhibit a rather restricted range of Nd and Pb isotopic ratios consistent with their derivation from an ocean island-type mantle source, the composition of which includes the HIMU (high $^{238}U/^{204}Pb$) component characteristic of the Galápagos hotspot. In contrast, the 123 Ma Ecuadorian oceanic rocks have flat REE patterns and (relative to NMORB) are depleted in Zr, Hf, Th, and U. Moreover, they show a wide range of Nd and Pb isotopic ratios intermediate between those of ocean island basalts and NMORB. It is unlikely, on geochemical grounds, that the plume source of the Ecuadorian fragments was similar to that of the Galápagos. In addition, because of the NNE motion of the Farallon plate during the Early Cretaceous, the Ecuadorian oceanic plateau fragments could not have been derived from the Galápagos hotspot but were likely formed at a ridge-centered or near-ridge hotspot somewhere in the SE Pacific.

1. Introduction

Oceanic plateaus originate by the outpouring of large volumes of mafic magmas over oceanic crust coupled with cogenetic plutonic intrusions. Despite their volumetric importance, little is known about their overall structure and composition, especially of their deeper crustal levels. Because of their thickness, they tend to be more buoyant than normal oceanic crust [*Burke et al.*, 1978; *Nur and Ben Abraham*, 1982; *Cloos*, 1993; *Saunders et al.*, 1996] and are not easily subducted. Therefore these oceanic plateaus can potentially be obducted onto, or accreted to, continental margins [*Ben Abraham et al.*, 1981], thus increasing both the probability of

[1]UPRESA 5025 CNRS, Université Joseph Fourier, Grenoble, France.
[2]UMR 5567-CNRS, Université Montpellier II, Montpellier, France.
[3]UMR-6526 CNRS, Université de Nice Sophia-Antipolis, Valbonne, France.
[4]UMR 5563-CNRS, Université Paul Sabatier, Toulouse, France.
[5]UMR 6538-CNRS, Université de Bretagne occidentale, Brest, France.
[6]Université de Lausanne, Lausanne, Switzerland.
[7]ORSTOM, Paris, France.
[8]UPRESA 5025 CNRS, Université de Savoie, Chambéry, France.
[9]Laboratoire de Pétrologie, Université Henri Poincaré, Vandoeuvre lès Nancy, France.

preservation and accessibility of their plutonic roots. Numerous accreted oceanic crustal fragments composed of ultramafic-mafic cumulate rocks, diabases, and basalts are exposed along the Pacific coast of Central America (Costa Rica) and South America (Colombia, Ecuador) and in the Caribbean (Venezuela, Greater Antilles, Aruba, Curaçao; Figure 1). Their origin, age, and emplacement are still a matter of ongoing debate. Age estimates of these complexes range from Late Jurassic to Paleocene. They are interpreted as being parts of a large basaltic province, the Caribbean-Colombian Igneous Province [*Kerr et al.*, 1997a, b].

The Late Cretaceous Caribbean basaltic crust drilled during the Deep Sea Drilling Project (DSDP) Leg 15 [*Donnelly et al.*, 1973] and Ocean Drilling Project (ODP) Leg 165 [*Sigurdsson et al.*, 1997] is enriched in large ion lithophile elements (LILE) and has relatively radiogenic (Sr and Pb) isotopic characteristics [*Sen et al.*, 1988] which are consistent with derivation from a similar mantle source as that of the Galápagos hotspot. Since diabases and basalts of oceanic fragments in the islands and continent bordering the Caribbean have geochemical characteristics similar to those of the drilled rocks, *Donnelly et al.* [1990] considered these rocks to represent uplifted parts of the Caribbean-Colombian Oceanic Plateau (CCOP). Using a fixed hotspot reference frame, *Duncan and Hargraves* [1984] suggested that the CCOP was produced during the initial "plume head" phase of the Galápagos hotspot.

The CCOP is mostly made of Upper Cretaceous diabases, shallow basaltic sills, or pillowed and/or massive flows of

Figure ... hematic map showing the location of the Mesozoic oceanic plateau crustal fragments exposed in ... al Mexico, Costa Rica, Greater Antilles, Curaçao, Aruba, Colombia, and western Ecuador.

North and South American cratons

Continental margins deformed during the Mesozoic and Tertiary

Undifferentiated terranes

OCEANIC PLATEAUS

Late Jurassic - Early Cretaceous (≥ 105 Ma)

Early Late Cretaceous (≡ 90-85 Ma)

Late Cretaceous (78-75 Ma)

1 : Arperos oceanic suture (Mexico)
2 : Dumisseau Formation (Southern Haiti)
3 : Duarte Complex (Dominican Republic)
4 : Curaçao Island
5 : Nicoya peninsula
6 : Volcanic Formation (Western Cordillera of Colombia)
7 : Amaime Formation of the suture zone of Colombia
8 : Gorgona Island
9 : Piñon Formation (
10 : Serrania de Baud

basalts, the latter being often picritic [*Donnelly et al.*, 1973]. Exposures of these lavas are reported in southern Haiti, Curaçao, and western Colombia (including the komatiites and enriched basalts from Gorgona Island) [*Aitken and Echeverria*, 1984; *Arndt et al.*, 1996; *Kerr et al.*, 1996a, 1997a]. *Kerr et al.* [1996a, b, c, 1997a] demonstrated that the enriched tholeiites (including komatiites) from Gorgona, Curaçao, and Colombia (with the exception of the Central Cordillera [*Kerr et al.*, 1997a]) are Upper Cretaceous in age (73-91.7 Ma) and likely derived from the Galápagos hotspot. Recent Ar/Ar ages and Sr, Nd, and Pb isotopic data indicate that the enriched basalts of the Nicoya Complex from Costa Rica, now considered to be the westernmost occurrence of the CCOP, are early Late Cretaceous in age (88-92 Ma) and can also be genetically linked to the Galápagos plume [*Alvarado et al.*, 1997; *Hauff et al.*, 1997; *Sinton et al.*, 1997]. Recently, *Sinton et al.* [1998] demonstrated on the basis of ^{39}Ar/^{40}Ar ages that the igneous rocks of the CCOP were emplaced during two main events: 90-82 Ma and 78-68 Ma. The rocks related to the early Late Cretaceous event (90-83 Ma, specifically Turonian to Santonian) were produced by a hotspot that possibly was the Galápagos, while those emplaced during the Late Cretaceous (78-68 Ma) possibly derived from a more depleted plume source.

Exposures of mafic plutonic and volcanic rocks with enriched tholeiitic affinities exposed in western Ecuador (Piñón Formation, see Figures 1 and 3) (C. Reynaud et al., Oceanic plateau and island arcs of southwestern Ecuador: Their place in the geodynamic evolution of northwestern America, submitted to *Tectonophysics*, 1998, herein after referred to as Reynaud et al., submitted manuscript, 1998) have also been assigned to the CCOP [*Kerr et al.*, 1996b, 1997a]. However, these rocks are older than those from most of the CCOP, since they are locally overlain by early Late Cretaceous ($\approx$ 95-90 Ma) sediments [*Jaillard et al.*, 1995; Reynaud *et al.*, submitted manuscript, 1998]. Furthermore, in the Central Cordillera of Colombia, part of the accreted fragments of an oceanic plateau were affected by Early Cretaceous high-pressure metamorphism (K/Ar ages [*Toussaint and Restrepo*, 1994]) and are older than 120 Ma. Finally, the enriched tholeiites of the Arperos basin exposed in central and western Mexico (Figure 1) [*Freydier et al.*, 1996], are geochemically similar to those of western Ecuador (see below). Moreover, they share with the rocks of western Ecuador similar Early Cretaceous age because they are stratigraphically interbedded with cherts that yielded Lower Cretaceous radiolarian faunas [*Dávila Alcocer and Martínez Reyes*, 1987].

There is presently some geochemical data (age, major, trace element, and Nd, Sr, and Pb isotopic compositions) on oceanic plateau basalts, for example, the Ontong Java plateau basalts exposed in the Solomon Islands [*Tejada et al.*, 1996] and the Upper Cretaceous komatiitic and picritic basalts from the Caribbean and northern South America. However, most of these exposures are still restricted to the volcanic levels of oceanic plateau crust, and none of them allows investigation to be made of the geochemical features of the underlying ultramafic and mafic plutonic roots of the oceanic plateau. The oceanic crustal fragments from Hispaniola and more specifically from Ecuador offer the unique opportunity to study different components of the CCOP, i.e., the Upper Jurassic oceanic crust basement and the Cretaceous ultramafic and mafic hypabyssal and volcanic rocks and their plutonic roots.

Major and trace element compositions and isotopic data, although necessary, cannot identify the parental hotspot(s) of these oceanic plateau magmas. Ages and transport directions of the allochthonous oceanic crustal fragments together with kinematics of regional plates are also required to constrain parental hotspot location.

The purpose of the present paper is to report new data on the trace element and isotopic (Sr, Nd, Pb) characteristics of selected clinopyroxene- and/or olivine-rich basalts of the Duarte Complex (Dominican Republic) and plutonic and volcanic rocks from coastal Ecuador. From the comparison of these data with our published data on basalts and diabases from westerncentral Mexico and those already available in the literature, we propose a new interpretation of the origin of the Caribbean-Colombian Oceanic Plateau.

2. Geological Information

2.1. Dominican Republic

The Duarte Complex forms the core of the Central Cordillera of the Dominican Republic. It is bounded on both sides by arc-derived rocks of Cretaceous age and intruded by Late Cretaceous to Tertiary plutons (Figure 2) [*Kesler et al.*, 1977]. *Bowin* [1975] and *Palmer* [1979] proposed that this complex represents a fragment of oceanic crust. *Draper and Lewis* [1991] and *Lewis and Jiménez* [1991] consider this complex to be a Late Jurassic-Early Cretaceous ocean island or seamount modified by Late Cretaceous-Eocene island arc magmatism [*Bowin*, 1966; *Kesler et al.* 1977; *Mercier de Lépinay*, 1987; *Draper and Lewis*, 1991]. *Donnelly et al.* [1990 p. 347] consider the picrites, ankaramites, and amphibolites of the Duarte Complex and the Upper Cretaceous unmetamorphosed mafic rocks of the Siete Cabezas to represent the "tectonized allochthon of the Caribbean Cretaceous basaltic rocks."

Detailed field mapping in the Juncalito-Janico-La Vega area allowed us to distinguish four units in the Duarte Complex (Figure 2), the first three of which are particularly important geochemically in the context of the present study: (1) a thick pile of Mg-rich basalts, (2) mafic amphibolites and amphibole-epidote gneisses tectonically imbricated with the Mg-rich basalts, (3) pillowed and massive basalts stratigraphically associated with Upper Jurassic (160-149 Ma) ribbon cherts [*Montgomery et al.*, 1994], and (4) serpentinized peridotites crosscut by diabase dikes.

The olivine and clinopyroxene (cpx)-rich basalts are metamorphosed to greenschist facies and are generally intensively deformed. However, the stratigraphic bedding marked by the flow contacts and the graded bedding in the pyroclastic levels are locally preserved, and the plagioclase-free, Mg-rich lavas form massive flows, < 2 m thick, interbedded with lapilli and crystal tuffs. These flows show evidence for accumulation of olivine and clinopyroxene crystals at their base, while their tops are highly vesicular. They are often intruded by diabase dikes. In the southeastern extremity of the Central Cordillera (Figure 2) the amphibolites of the Duarte Complex are tectonically overlain by the unmetamorphosed diabases, basalts, and cherts of the Siete Cabezas Formation containing Cenomanian to Santonian (97-83 Ma [*Gradstein et al.*, 1994]) radiolarians [*Mercier de Lépinay*, 1987; *Donnelly et al.*, 1990].
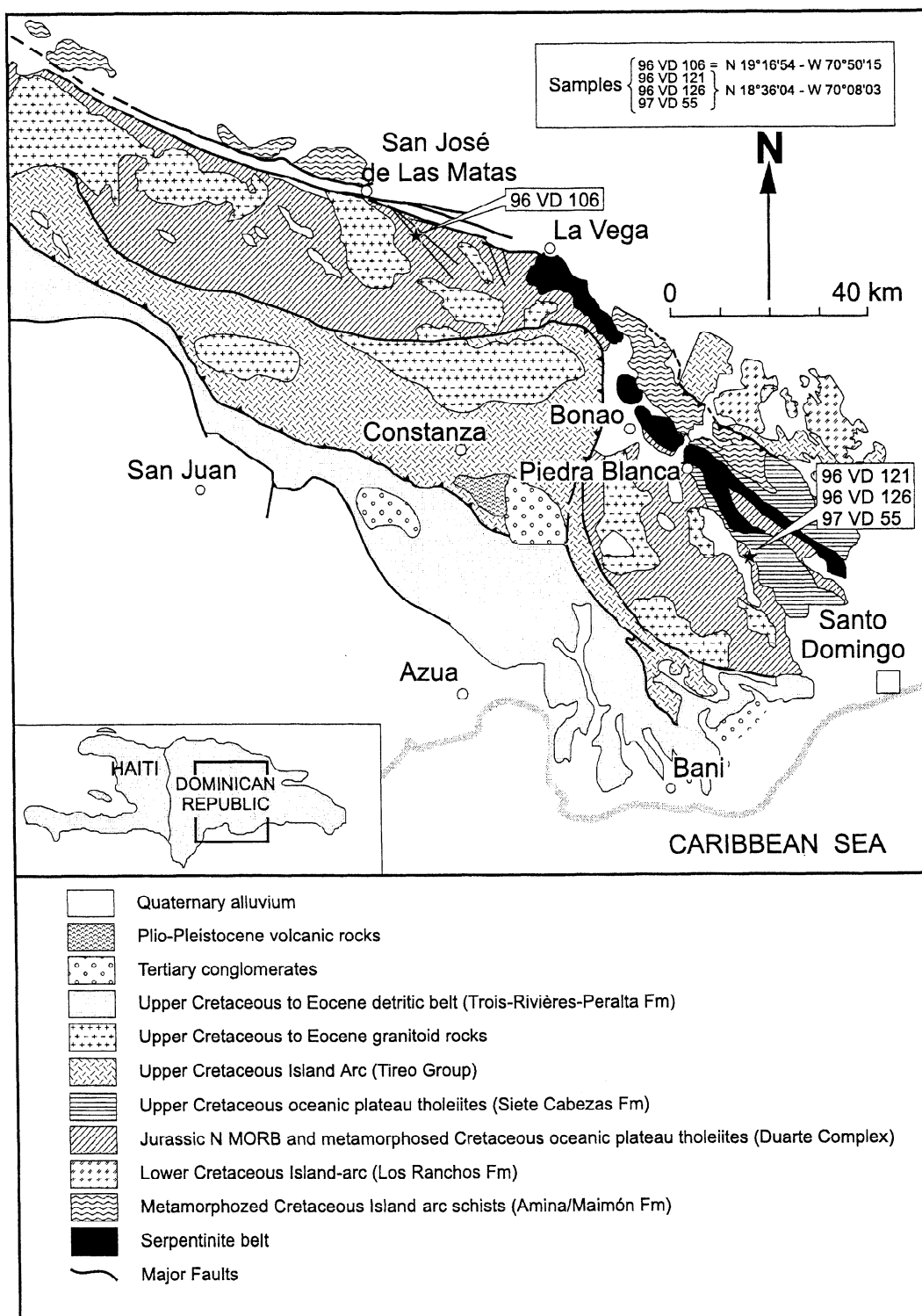
Figure 2. Schematic map of the Duarte Complex in the Central Belt from Dominican Republic showing the location of the analyzed samples discussed in the text.

Ar/Ar ages of 86 ± 1.4 Ma of both late magmatic amphibole (magnesio-hastingsite) from a cumulus-enriched rock and of hornblende from an amphibolite (96VD126, see below) [*Lapierre et al.*, 1999] indicate that the Mg-rich lavas and amphibolites of the Duarte Complex are contemporaneous with the oceanic plateau tholeiites of the CCOP exposed in the Caribbean and Central America.

2.2. Ecuador

Three main geological domains can be distinguished (Figure 3). The NNE trending Andean Cordillera is predominantly composed of deformed Paleozoic to Mesozoic metamorphic rocks [*Aspden and Litherland*, 1992; *Noble et al.*, 1997] crosscut and overlain by the products of Tertiary magmatic
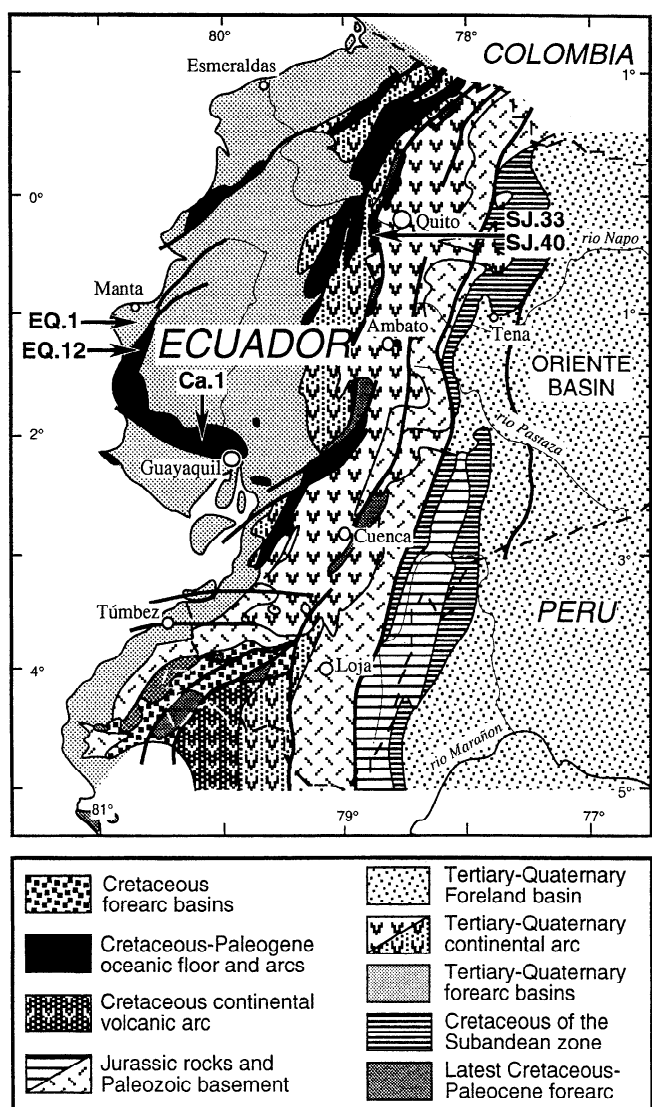
Figure 3. Schematic map of Ecuador showing the location of the analyzed samples discussed in the text.

arcs [*Aspden et al.*, 1992; *Lavenu et al.*, 1992]. Cretaceous to Paleogene continental volcanic arcs cropping out in southwestern Ecuador represent the continuation of the magmatic arc of Peru [*Jaillard et al.*, 1996].

The western coastal zone comprises an oceanic igneous basement, unconformably overlain by early Late Cretaceous to Paleogene intraoceanic arcs [*Lebrat et al.*, 1987; *Bourgois et al.*, 1990; R. Marksteiner and A. Alemán, unpublished report, 1991], in turn, overlain by Tertiary forearc marine sediments. The igneous basement (i.e., the Piñón Formation) consists of pillow basalts and diabases which yielded dubious K/Ar ages on plagioclase and whole rocks ranging from 110 to 54 Ma [*Goossens and Rose*, 1973]. This basement is stratigraphically overlain by undated volcanic rocks of oceanic arc origin, which are in turn overlain by pelagic sediments containing Cenomanian(?) to Turonian faunas. Thus the age of the oceanic basement of Coastal Ecuador can be regarded as pre-early Late Cretaceous.

In the eastern part of the coastal zone (i.e., the Western Cordillera) the Cretaceous-Paleogene magmatic rocks are in fault contact with the basement of the Andean Cordillera. Tectonic slices of ophiolitic series pinched along this contact were interpreted as remnants of an oceanic crust [*Juteau et al.*, 1977; *Lebrat et al.*, 1987] or an oceanic plateau [*Desmet*, 1994]. The island arcs and their oceanic basement were accreted to the margin of the South American Plate during Late Cretaceous to late Paleocene times [*Jaillard et al.*, 1996; *Cosma et al.*, 1998]. In summary, coastal Ecuador is a fragment of oceanic lithosphere of pre-Late Cretaceous age (> 91 Ma), overlain by early Late Cretaceous to Tertiary intraoceanic volcanic arc series.

2.3. Western Central Mexico

The Guerrero volcano-plutonic arc was accreted to the continental margin of western Mexico before Cenomanian times [*Tardy et al.*, 1986]. It is presently separated from the Precambrian and Paleozoic terranes of Mexico by the Arperos oceanic suture (Figure 4). In northwestern and central Mexico the Arperos suture contains scattered outcrops of submarine mafic lava flows and diabases overlain by pelagic sediments containing Early Cretaceous radiolarian fauna [*Dávila Alcocer and Martínez Reyes*, 1986].

3. Analytical Procedures

Diabases, and cpx- and/or olivine-rich basalts experienced hydrothermal alteration and metamorphism up to the greenschist facies. Accordingly, only those samples with well-preserved original igneous mineralogy (i.e., clinopyroxene, amphibole, and plagioclase phenocrysts) and devoid of any significant petrographic alteration features were selected for study. Phenocrysts were separated then purified by hand picking. The petrographic features of these rocks are summarized in Table 1. However, actinolite rims around some cpx crystals could not be completely removed.

For Sr and Nd isotopic analyses, mineral separates and host rock powders were leached in a $2 N$ HCl-0.1 N HF mixture. For Pb isotope determinations, mineral separates and whole rocks were successively leached in hot $2 N$ HCl for 20 min in an ultrasonic bath, rinsed with tridistilled water, leached in cold 1 N HNO₃ for 20 min, and rinsed with tridistilled water in an ultrasonic bath for 15 min.

Trace elements were analyzed by inductively coupled plasma mass spectrometry (ICP-MS) at the University of Grenoble after acid dissolution. Rare earth element (REE) were first separated as a group and spiked with pure Tm using procedures described by *Barrat et al.* [1996]. Standards used for the analyses were JB2, WSE BIR-1, JR1, and UBN (Table 2). Major element analyses were performed by ICP-optical emission spectroscopy at the Université de Bretagne Occidentale. Major and trace element analyses of the minerals and host rocks are presented in Table 2.

The $^{143}Nd/^{144}Nd$ and $^{87}Sr/^{86}Sr$ isotopic characteristics were determined on a Finnigan MAT261 multicollector mass spectrometer at the Laboratoire de Géochimie de l'Université Paul Sabatier (Table 3), using the analytical procedures of *Lapierre et al.* [1997]. The $^{206}Pb/^{204}Pb$, $^{207}Pb/^{204}Pb$ and $^{208}Pb/^{204}Pb$ isotopic ratios were measured on a multicollector VG sector mass spectrometer at the Laboratoire de Géochimie isotopique de l'Université de Montpellier II (Table 3)
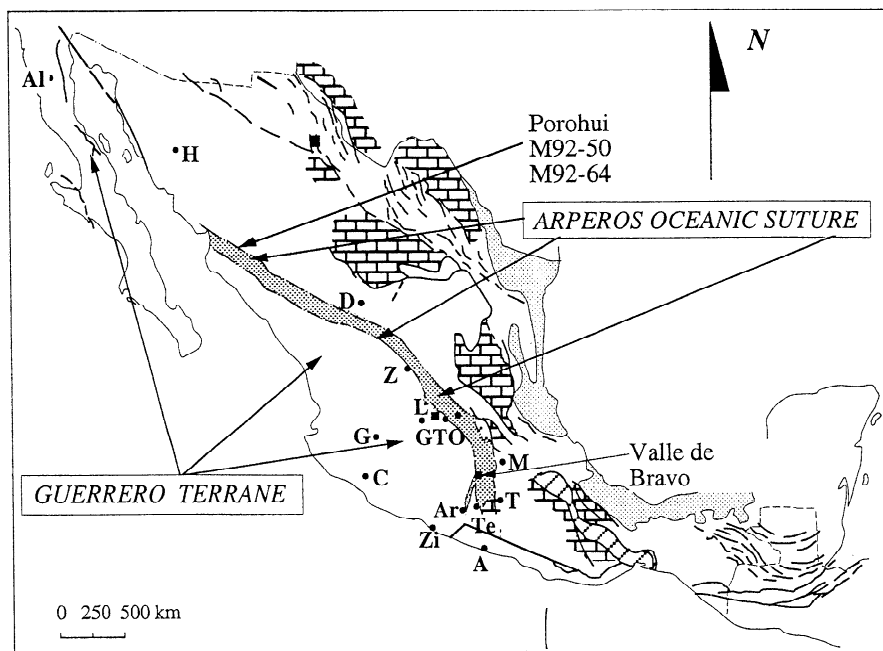
Figure 4. Schematic map of the Arperos basin and the Guerrero terrane showing the location of the samples quoted in the text. A, Acapulco; Al, Alisitos; Ar, Arcelia; C, Colima; D, Durango; G, Guadalajara; GTO, Guanajuato; H, Hermosillo; L, Leon; M, Mexico city; T, Taxco; Te, Teloloapan; Z, Zacatecas; Zi, Zijuatanejo.
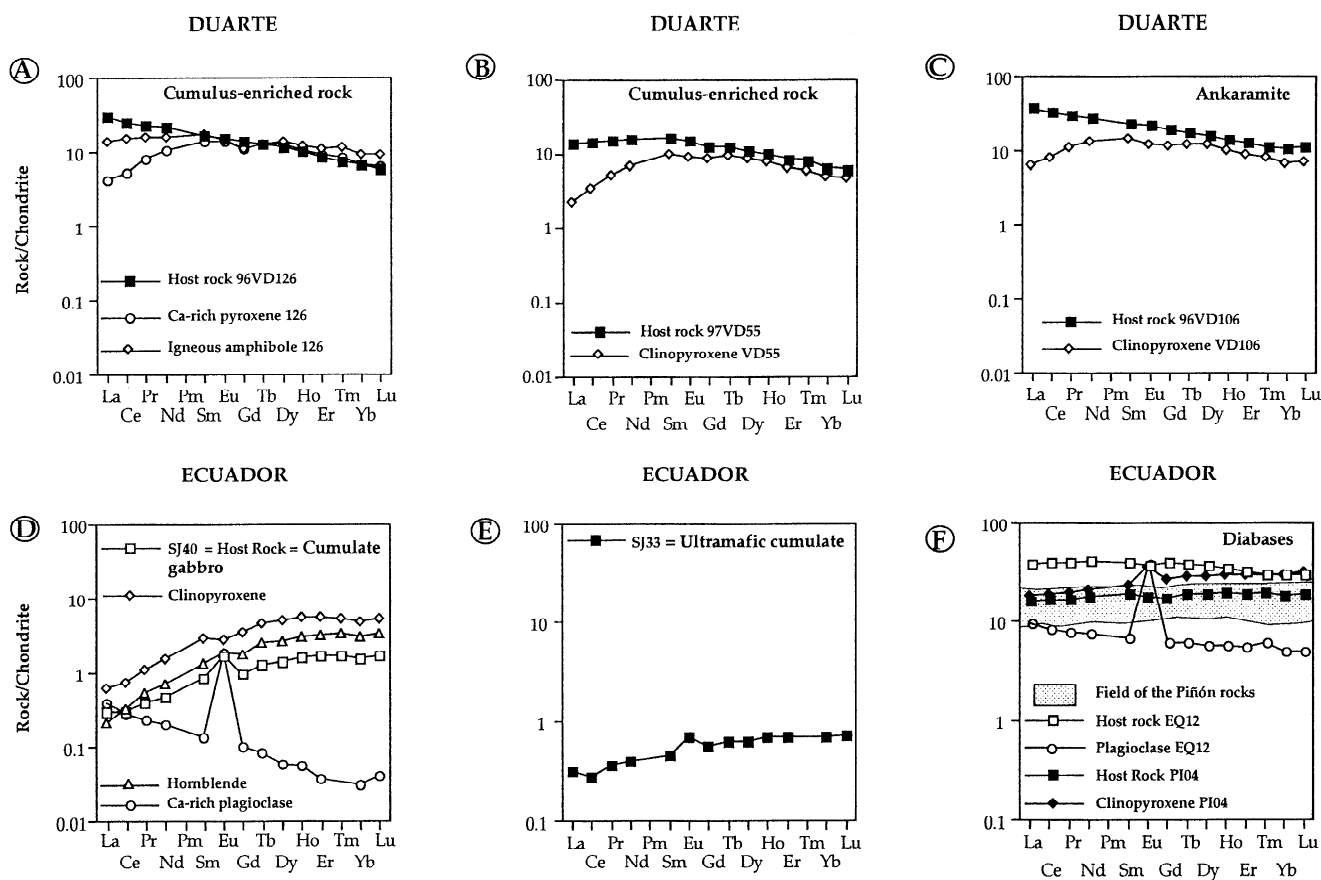
Figure 5. Chondrite-normalized (N) rare earth element patterns of the minerals and host rocks which show oceanic plateau affinities. San Juan cumulates and Piñón diabases are from Ecuador. Cumulus-enriched picrites and ankaramites belong to the Duarte Complex from Dominican Republic. Chondrite values are from *Sun and McDonough* [1989].

Table 1. Location and Descriptions of Duarte Complex (Dominican Republic), Piñón Formation (Ecuador), and Arperos Formation (Mexico) Samples

Duarte Complex	Sample			
	96VD126	97VD55	96VD121	96VD106
	Villa Altagracia Autopista Santo Domingo	Villa Altagracia Autopista Santo Domingo	Villa Altagracia Autopista Santo Domingo	South Janico road to Juancalito
Texture	cumulus-enriched	cumulus-enriched	porphyritic	porphyritic
Mineralogy	olivine pseudomorphs (5%) large cpx phenocrysts (80%) rimmed by Mg-rich Hastingsite (3%) skeletal cpx crystals interstitial glass (12%) present recrystallized to smectites	cpx large crystals (90%) interstitial glass (10%) present, recrystallized to smectites	cpx large crystals (60%) rimmed locally by actinolitic hornblende glassy groundmass (40%)	cpx large crystals (30%) in a quenched groundmass (70%) with skeletal cpx microlites glass recrystallized to smectites
Name	cpx-rich cumulative basalt	cpx-rich cumulative basalt	cpx-rich basalt	cpx-rich basalt

Ecuador	Sample			
	SJ40	SJ33	EQ12	PIO4
	Quebrada San Juan	Quebrada San Juan	Puerto Cayo	North of Guayaquil
Texture	adcumulate layered	cumulus layered	ophitic	intersertal
Mineralogy	preserved plagioclase (70%) cpx (25%) partly transformed to hornblende opx (5%) pseudomorphs	cumulus: olivine (60%) + cpx (35%) intercumulus: anorthite (5%)	plagioclase laths (50%) interstitial cpx (40%) Fe-Ti oxides (10%)	plagioclase laths (50%) cpx (40%) epidote + chlorite (10%)
Name	gabbro	wehrlite	diabase	diabase

Western Mexico Arperos	Sample		
	M93-17	M92-50	M92-64
	Valle de Bravo	Porohui	Porohui
Texture	porphyritic		intersertal
Mineralogy	skeletal olivine (5%) replaced to calcite + Crspinels quenched Ti-rich cpx (15%) oxides (5%) in the groundmass (75%)	plagioclase (40%) laths and phenocrysts replaced to albite small cpx crystals (20%) groundmass (40%)	plagioclase (40%) laths and microlites cpx (20%) calcite-filled vesicles (20%) groundmass (40%)
Name	basalt	basalt	basalt

Table 2. Major and Trace Element Analyses for the Duarte Complex and Ecuadorian Minerals and Host rocks, and Arperos Basalts

	Ecuador SJ40 Cpx	Ecuador SJ40 Amphibole	Ecuador SJ40 Plagio	Ecuador RTSJ40 Cumulate Gabbro	Ecuador SJ33 Cumulate Peridotite	Ecuador SJ33 Duplicate	Standard UBN Ultramafic	Ecuador PI04 cpx	Ecuador PI04 RT Intersertal Diabase	Ecuador EQ12 Plagio	Ecuador EQ12 Ophitic Diabase	Duarte 97VD55* cpx	Duarte 97VD55 RT Cumulus-enriched	Duarte 96VD126* Amphibole	Duarte 96VD126 cpx	Duarte 96VD126 RT Cumulus enriched	Duarte 96VD106* cpx	Duarte 96VD106 cpx rich basalt	Arperos M93-17 Basalt	Arperos M92-50 Basalt	Arperos M92-64 Basalt
SiO_2				49.61	42.96				53.32	42.89	54.2	51.4	48.86	38.23		46.5	50.1	45.5	44.5	43.48	44.1
TiO_2				0.07	0.04				1.48		2.1	0.65	1.04	2.96		1.5	1	1.46	0.9	1.79	2.1
Al_2O_3				16.33	6.55				13.59		13.34	3	8.04	12.3		10.79	3.9	11.55	15.1	14.06	16.5
Fe_2O_3				6.32	12.68				15.04		16.64	6.8*(a)	11.0	16.93*(a)		13.11	6.52*(a)	12.17	8.4	7.32	10.74
MnO				0.08	0.16				0.22		0.23	0.17	0.17	0.26		0.18	0.12	0.2	0.1	0.16	0.1
MgO				12.48	32.55				6.55		3.1	16	13.72	9.83		11.25	14.45	9.65	6.4	4.61	8
CaO				14.88	6.12				8		5.79	20.37	14.63	11.72		12.2	22.5	10.5	12.6	14	6.3
Na_2O				0.74	0.08				3.19		4.09	0.27	0.85	2.88		2.09	0.42	0.73	4.1	3.5	3.7
K_2O				0.04	0.01				0.01		0.13	bdl	0.12	0.48		0.1		0.12	0.2	0.28	1.2
P_2O_5											0.29	bdl	0.07	bdl		0.15		0.36	0.1	0.27	0.4
LOI												bdl	bdl	bdl		2.38		4.71	7.4	10.42	7.2
Total												98.66	98.51	95.6		100.25	99.01	99.95	99.8	99.89	100.34
Ba, ppm	8.306	2.87	4.69	9.24	4.75	6.46	31.36	4.47	14.50	na	na	2.571	23.708	31.2	8.96	100	5.52	106	38.51	88.31	426
Cr	na	na	na	172	2480	na	na	na	58	na	bdl	na	1925	na	na	1050	na	460	287	286	217
Hf	bdl	bdl	bdl	bdl	bdl	bdl	0.13	bdl	2.10	1.11	2.49	bdl	bdl	3.04	bdl	bdl	bdl	2.7	3.84	3	4.75
Nb	0.117	0.30	0.35	bdl	bdl	bdl	0.06	1.58	4.74	bdl	10.75	1.526	3.71	12.7	3.66	bdl	0.79	15.46	10.06	6.91	9.78
Ni	na	na	na	98	962	na	na	na	69	na	na	na	268	na	na	454.91	na	215.23	146	129	50
Rb	0.16	0.16	0.19	0.34	0.21	0.16	2.91	0.099	0.24	0.89	1.61	0.34	1.815	0.51	0.29	0.63	0.52	2.98	1.45	2.32	14.2
Sr	7.50	6.41	215.87	86.61	23.32	21.73	7.68	43.66	46.21	174	116.12	19.83	114.78	120.9	34.9	53.06	53.2	392.47	249	308	391.5
Ta	bdl	bdl	bdl	bdl	bdl	bdl	0.018	0.106	0.38	bdl	0.67	bdl	0.23	0.69	0.2	bdl	0.05	1.01	0.68	0.46	0.6
V	na	na	na	99	45	na	na	45.74	359	na	na	na	455.5	na	na	272.94	na	262.63	204	239	278
Y	7.64	3.83	0.07	2.16	1.03	0.89	2.33	bdl	28.09	9.95	51.02	10.06	13.18	17.8	14.1	9.57	13.9	18.49	33.35	25.57	28.3
Zr	bdl	bdl	bdl	bdl	0.58	0.41	3.13	0.035	66.05	41.65	77.07	bdl	na	83.8	bdl	bdl	bdl	88.47	172.8	117	170
Pb	bdl	bdl	bdl	0.60	bdl	0.32	12.64	0.341	0.68	0.23	0.22	bdl	0.48	0.87	0.27	0.548	0.4	2.938	1.06	1.23	0.85
Th	bdl	bdl	bdl	bdl	bdl	bdl	0.07	0.08	0.33	0.17	0.43	bdl	0.234	0.28	0.06	0.66	0.05	0.74	0.76	0.54	0.62
U	bdl	bdl	bdl	bdl	bdl	bdl	0.07	0.08	0.09	0.15	0.11	bdl	0.08	bdl	bdl	0.11	bdl	0.16	0.3	0.56	0.38
La	0.139	0.044	0.089	0.068	0.073	0.068	0.31	4.316	3.756	2.32	9.25	0.508	3.042	3.16	0.98	6.98	1.49	8.97	10.76	7.3	8.54
Ce	0.424	0.183	0.168	0.175	0.166	0.155	0.749	11.422	9.992	5.17	24.49	2.016	8.156	8.86	3.12	15.06	4.75	19.57	26.78	19.66	24.02
Pr	0.103	0.045	0.021	0.036	0.033	0.029	0.107	1.827	1.555	0.75	3.8	0.46	1.316	1.47	0.73	2.12	1.01	2.76	3.87	3.06	3.61
Nd	0.69	0.325	0.092	0.206	0.184	0.175	0.569	9.571	8.04	2.23	19.53	3.019	6.908	7.38	4.72	9.89	5.94	12.64	17.5	14.31	17.43
Sm	0.431	0.187	0.02	0.122	0.069	0.077	0.2	3.494	2.818	1.06	6.11	1.408	2.332	2.54	2.00	2.5	2.15	3.46	4.8	4.1	4.64
Eu	0.156	0.099	0.102	0.096	0.039	0.042	0.077	2.022	1.06	2.23	2.19	0.484	0.801	0.82	0.79	0.84	0.68	1.24	1.59	1.34	1.40
Gd	0.689	0.368	0.003	0.193	0.113	0.117	0.317	5.003	3.412	1.29	8.37	1.666	2.38	2.25	2.2	2.83	2.32	3.88	5.2	4.24	5.56
Tb	0.17	0.079	0.003	0.046	0.023	0.024	0.059	1.079	0.709	0.23	1.47	0.329	0.432	0.45	0.45	0.47	0.44	0.63	0.93	0.74	0.89
Dy	1.25	0.604	0.014	0.35	0.165	0.164	0.406	7.514	4.783	1.47	9.56	2.026	2.561	3.42	3.06	2.81	2.94	3.89	5.58	4.45	5.62
Ho	0.3	0.146	0.003	0.088	0.038	0.038	0.096	1.774	1.107	0.33	1.96	0.414	0.538	0.68	0.58	0.56	0.56	0.78	1.23	0.95	1.13
Er	0.87	0.441	0.006	0.266	0.112	0.109	0.264	5.067	3.146	0.92	5.48	1.031	1.323	1.81	1.47	1.36	1.41	2.05	3.43	2.61	3.21
Tm	0.133	na	na	0.041	na	na	na	0.809	0.491	0.16	0.77	0.143	0.195	0.28	0.21	0.18	0.2	0.27	0.51	0.39	0.42
Yb	0.795	0.473	0.005	0.256	0.115	0.111	0.29	5.109	3.088	0.85	5.17	0.8	1.067	1.53	1.12	1.09	1.12	1.77	3.19	2.37	2.79
Lu	0.13	0.074	0.001	0.041	0.018	0.019	0.048	0.836	0.477	0.126	0.77	0.114	0.15	0.23	0.16	0.14	0.17	0.27	0.49	0.36	0.41
$(La/Yb)_N$	0.12	0.06	11.57	0.19	0.45	0.45	0.61	0.61	0.87	1.94	1.28	0.455	2.04	1.48	0.62	4.31	0.95	3.41	2.42	2.10	2.19

Locations, samples, facies, and rock types are given. Limits of detection: Zr = 24 ppb, Nb = 5 ppb, Ta = 0.5 ppb, Hf = 1 ppb, U, Th and Pb = 0.6 ppb.

*Analytical conditions of microprobe analysis. 15 kV, 10-20 nA, focused beam, natural standards.

(a)Major elements reported on volatile free basis after Desmet [1994] and Reynaud et al. (submitted, manuscript, 1988). na, not analyzed. bdl, below detection limit.

#Zoned cpx, mean analysis is without signification. Microprobe analyses of major elements are available on request.

Table 3. Nd, Sr, and Pb Isotopic Analyses for the Duarte Complex, Ecuadorian, and Mexican Minerals and Host Rocks

Facies	$(^{206}Pb/^{204}Pb)_i$	$(^{207}Pb/^{204}Pb)_i$	$(^{208}Pb/^{204}Pb)_i$	$^{143}Nd/^{144}Nd$	$^{87}Sr/^{86}Sr$	$(^{87}Sr/^{86}Sr)_i$	εNd	εSr	
Cumulate 96VD126	19.094	15.550	38.603	0.513051 ± 4	0.703190±6	0.70315	+8.53	-17.77	Duarte
Amphib. 126	19.158	15.601	38.956	0.513054 ± 6	0.703163 ±18	0.70315	+7.99	-17.77	85 Ma
Cpx - 126				0.513100 ± 6	0.703233 ±13	0.70320	+8.34	-16.98	Hispaniola
Ankaramite 96VD106	19.537	15.588	39.188	0.512951 ± 4	0.703520 ± 8	0.70349	+6.45	-12.87	
Cpx 106	19.252	15.557	38.941	0.512957 ± 7	0.703642 ± 12	0.70362	+5.52	-11.06	
Cumulate 96VD121	19.146	15.525	38.800	0.512936 ± 8	0.703867± 25	0.70370	+6.19	-9.95	
Amphib. 121	19.466	15.563	39.267						
Cumulate 97VD55	18.966	15.565	38.621	0.512979 ± 9	0.703234 ± 8	0.70318	+6.57	-17.34	
Cpx 55				0.513073 ± 7	0.703270 ± 18	0.70321	+7.56	-16.89	
Pillow basalt M92-50	18.712	15.563	38.168	0.512997 ± 36	0.704372 ± 11	0.70432	+7.2	-0.72	Arperos
Pillow basalt M93-17	18.271	15.570	37.948	0.513027 ± 13	0.704435 ± 11	0.70432	+8.2	-0.70	110 Ma
Pillow basalt M92-64	18.304	15.558	38.099	0.512912 ± 48	0.704720 ± 8	0.70455	+5.8	+2.49	Mexico
Diabase PiO4	17.898	15.595	37.825	0.513008 ± 6	0.703506 ± 11	0.70348	+6.98	-12.43	Piñon
Cpx PiO4				0.513043 ± 6	0.703588 ± 10	0.70358	+7.53	-11.06	123 Ma
Diabase EQ12	17.414	15.548	37.166	0.513026 ± 6	0.703561 ± 12	0.70349	+7.69	-12.27	Ecuador
Plagio. EQ12				0.512055 ± 30	0.703327 ± 21				
Diabase EQ1	18.159	15.529	37.840	0.513154 ± 25	0.703451 ± 27	0.70321	+10.1	-16.24	
Diabase CA1	18.923	15.566	38.431	0.512870 ±7	0.704542 ± 17	0.70435	+4.49	-0.03	
Gabbro SJ40	18.193	15.602	38.100						
Plagio. SJ40	18.126	15.473	37.890	0.512822 ± 18	0.703162 ± 7	0.70316	+4.62	-17.01	
Cpx. SJ40				0.513079 ± 11	0.703588 ± 10	0.70348	+5.84	-12.44	
Amphib. SJ40				0.513046 ± 16	0.703473 ± 20	0.70335	+5.59	-14.33	
Ultramafic SJ33				0.512822 ± 14	0.703448 ± 13	0.70282	+3.17	-13.10	

Pb isotope ratios were corrected with a mass discrimination factor of 0.13% per atomic mass unit relative to values of the NBS-981 standard measured during this period: $^{206}Pb/^{204}Pb = 16.936 \pm 0.006$, $^{207}Pb/^{204}Pb = 15.494 \pm 0.006$ and $^{208}Pb/^{204}Pb = 36.721 \pm 0.013$. Pb isotope ratios 2σ uncertainties are assumed to be less than 0.15%.

Table 4. Sm and Nd Contents and ^{143}Nd/^{144}Nd Ratios From SJ13 Whole Rock, Amphibole, and Plagioclase Concentrates

Sample	Nd, ppm	Sm, ppm	^{147}Sm/^{144}Nd	^{143}Nd/^{144}Nd
SJ13 whole rock	8.40	2.68	0.193	0.513008±29
SJ13 plagioclase	0.99	0.18	0.108	0.512962±08
SJ13 amphibole	27.59	9.63	0.211	0.513045±04

The Sm and Nd concentrations have been determined by isotope dilution using a mixed ^{149}Sm and ^{146}Nd enriched solution. Sm/Nd errors are 1%

following the analytical procedure adapted from *Manhès et al.* [1980]. Total Pb blanks are less than 65 pg for a 100 mg sample.

Isotopic data on minerals and host rocks have been corrected for in situ decay with an age of 86 Ma (Dominican Republic samples) and 123 Ma (Ecuador samples). This is based on Ar/Ar ages measured on Duarte igneous amphiboles [*Lapierre et al.*, 1999] and on a Sm/Nd internal isochron age determined on a gabbro from Ecuador, respectively (Table 4).

4. Trace Element Chemistry on Mineral Separates and Their Host Rocks

4.1. Dominican Republic

REE patterns of samples 96VD126 (olivine and cpx-rich basalt) and 96VD106 (cpx-rich basalt) are light REE (LREE)-enriched (3.4 <(La/Yb)$_N$< 4.3; Table 2 and Figure 5) with low REE contents (around 10 times chondritic values). These data are in agreement with previous works [*Kerr et al.*, 1996b, 1997a]. Sample 97VD55 (cpx cumulate) differs from the others, being less enriched in LREE ((La/Yb)$_N$= 2.04). Clinopyroxenes have very similar REE$_N$ patterns with moderate LREE depletions (0.45 < (La/Yb)$_N$< 0.95), whatever their host rock type. Amphiboles have rather flat REE patterns ((La/Yb)$_N$= 1.48). The LREE enrichment of whole rock with respect to clinopyroxene (cpx) and amphibole (amph) is consistent with the preferential partitioning of REE into the melt. The heavy REE (HREE) levels in the host rock and cpx are quite similar, with the exception of 96VD126 host rock which is more HREE-depleted than its cpx (Figure 5a).

Relative to normal mid-ocean ridge basalts (NMORB) (Figure 6), these rocks and their minerals show moderate enrichment in LILE and high Nb, Ta, and Pb contents. Their Th/U ratios (3.34 < Th/U < 6.75; Figure 7) fall within the range of the mid-Cretaceous tholeiites from Costa Rica [*Hauff et al.*, 1997; *Sinton et al.*, 1997]. In the cumulus-enriched rocks, trace element patterns of minerals and related host rocks are more or less parallel. This is not the case for the cpx-rich basalt where the host rock is markedly enriched in Th, Ta, and Nb with respect to the cpx. Pb has similar behavior in the cpx and in its host rock. This suggests that Nb, Ta, and Pb were concentrated in the groundmass.

The Duarte Mg-rich rocks show a wide range of Nb/U and Pb/Ce ratios (Figure 7) (29.9 < Nb/U < 96.6; 0.01 < Pb/Ce < 0.09) but with U contents significantly lower than those of ocean island basalts (OIB) (0.96 < U < 1.68). Th/U is higher and Nb/Ta and Zr/Hf are generally lower than NMORB (Figure 7).

4.2. Ecuador

The diabases of the Piñon Formation (Reynaud *et al.*, submitted manuscript, 1998) differ from the Duarte cpx-rich basalt in having flat REE patterns (0.87 < (La/Yb)$_N$ < 1.28; Table 2 and Figure 5). Compared to the host rock, PIO4 cpx has similar REE abundances but differs in the degree of LREE depletion ((La/Yb)$_N$ = 0.61) and is enriched in HREE. The EQ12 Ca-rich plagioclase REE concentrations are significantly lower than those of its host rock, and this mineral is LREE-enriched compared to the HREE ((La/Yb)$_N$ = 1.94; Table 2 and Figure 5).

The cumulate rocks from western Ecuador (SJ33, SJ40; Table 1) and SJ40 cpx differ from the Duarte cumulus-enriched rocks (96VD126, 97VD55) and related cpx in having significantly lower REE contents (Table 2; < 10 times the chondritic abundances) and a marked LREE depletion (Figure 5). The whole rock SJ40 and its related cpx and hornblende have similar parallel REE patterns, characterized by a significant LREE depletion (0.06 < (La/Yb)$_N$ = < 0.19; Figure 5 and Table 2). The cpx and its host rock have the highest and lowest REE levels, respectively, which are < 10 times the chondritic values. Hornblende has lower La and Ce abundances than the host rock. Ca-rich plagioclase is LREE-enriched ((La/Yb)$_N$ = 11.57; Table 2). Finally, the cumulate wehrlite is LREE-depleted ((La/Yb)$_N$ = 0.45) and has negative Ce (Ce/Ce* = 0.51) and positive Eu (Eu/Eu* = 1.24) anomalies.

Relative to NMORB, the Piñon diabases have high Nb, Ta, and Th values, characteristic of plume-generated magmas. Moreover, their Th/U ratios are slightly higher than those of NMORB (Table 2 and Figure 6) with the exception of EQ12. However, these rocks differ from the Duarte cumulus-enriched olivine and/or cpx-rich basalts by their lower contents of Zr, Hf, U, Th, Nb, and Ta (38.14 < Nb/U < 52; Table 2 and Figures 6 and 7). The Pb/Ce ratios of these rocks are low (0.008 < Pb/Ce < 0.07) with the exception of the cumulate gabbro (Pb/Ce = 3.45) but generally higher than those of MORB.
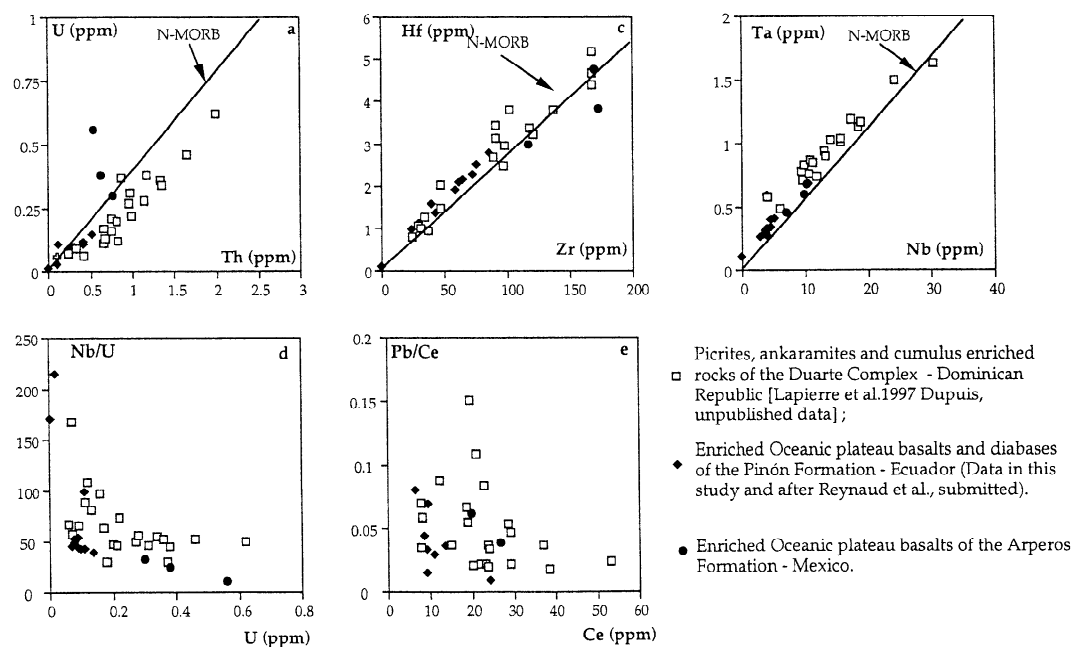
4.3. Western Mexico

The Arperos basalts presented here belong to group 1 [*Freydier et al.*, 1996]. They differ from the Piñon rocks by a greater LREE enrichment relative to HREE ((La/Yb)$_N$ ~ 2; Table 2 and Figure 8) which is nevertheless smaller than that of the Duarte cpx-rich basalts.

Relative to NMORB, the Arperos basalts are enriched in Th, U, Ta, and Nb but slightly depleted in Hf and Zr. Their U, Th, Hf, and Zr abundances are higher than those of the Piñon rocks and more or less similar to those of the Duarte cpx-rich basalts (Figure 6). In contrast, their Nb and Ta contents are intermediate between those of Piñon and Duarte rocks. Their Nb/U ratios (12.33 to 33.5) are lower than those of the Duarte and Piñon rocks (Figure 7). Their Pb/Ce ratios are low (0.045 and 0.062) but slightly higher than those of the Piñon rocks.
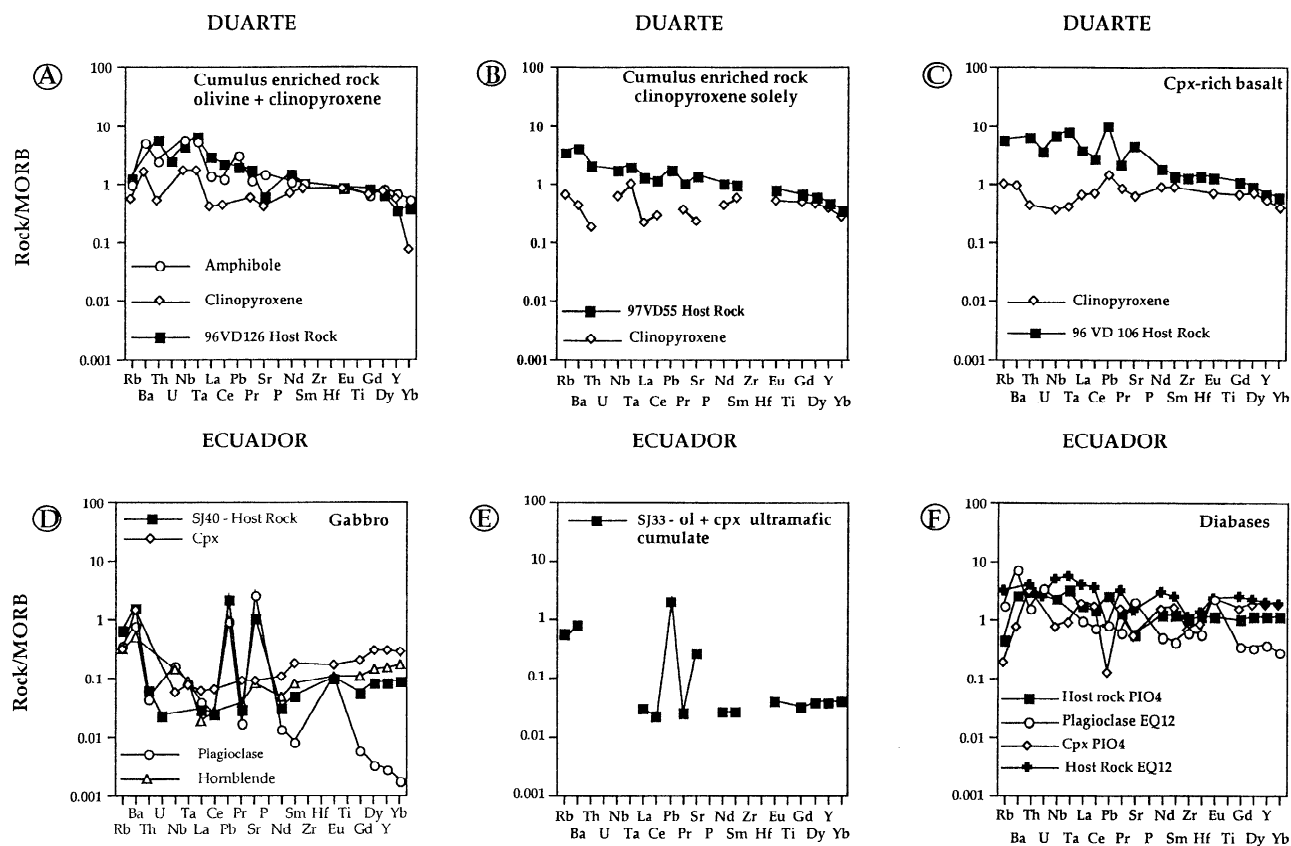
Figure 6. NMORB-normalized trace element patterns for the minerals and host rocks from Dominican Republic and Ecuador. NMORB values are from *Sun and McDonough* [1989].

Figure 7. U-Th, Hf-Zr, Ta-Nb, Nb/U-U, and Pb/Ce-Ce plots for the igneous rocks from Dominican Republic, Ecuador, and western Mexico.
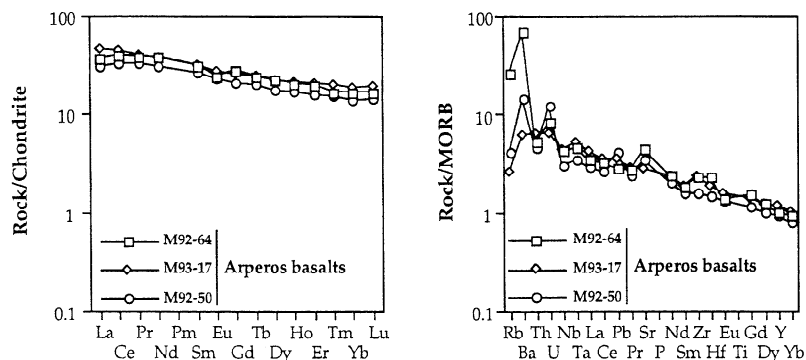
Figure 8. Chondrite-normalized (N) rare earth and NMORB normalized trace element patterns of the basalts of the Arperos Formation (westerncentral Mexico) which show oceanic plateau affinities. Chondrite and NMORB values are from *Sun and McDonough* [1989].

5. Characteristics of Calculated Melts in Equilibrium With cpx

In order to determine the compositions of the cpx parent magmas, REE compositions of melts in equilibrium with these minerals were calculated using the partition coefficients of *Hart and Dunn* [1993]. The REE abundances of these calculated melts based on 97VD55 and 96VD126 cpx compositions of the Duarte basalts (Figure 9) match well with those of the cpx-rich basalt 96VD106 (Figure 5a). The REE composition of the calculated melt based on 97VD55 cpx composition is rather similar to those of both cpx-rich basalts. The calculated melt in equilibrium with 96VD126 cpx composition has a similar LREE-enriched pattern associated with higher REE abundances and a positive Ce anomaly, which is absent in the Mg-rich rocks. The liquid in equilibrium with the 97VD55 cpx has a composition similar to that of the cpx-rich basalt (96VD106). The higher REE abundance of the calculated melt based on

96VD126 cpx is probably related to olivine crystallization leading to a more fractionated residual liquid in the cumulus-enriched rock.

The REE pattern of the calculated melt, based on the SJ40 cpx of the gabbro from Ecuador (using again partition coefficients from *Hart and Dunn* [1993] is more or less flat (Figure 9) and similar to those of the Piñon diabases (Table 2 and Figure 5b) but displays negative spikes for Ce and Nd which are absent in the REE patterns of the Piñon diabases. However, cpx SJ40 was probably in equilibrium with an enriched tholeiitic magma characterized by a flat REE pattern, similar to those of the Piñón diabases.

In summary, the rocks from Dominican Republic, Ecuador, and western Mexico have general oceanic plateau basalts affinities but show differences in trace element compositions. The Duarte Mg-rich rocks are enriched in LREE, Pb, Th, and U and are characterized by high Th/U ratios. Relative to NMORB, they are depleted in HREE and Y. In contrast, the Piñón diabases have flat REE patterns and are Pb, Zr, and Hf depleted.
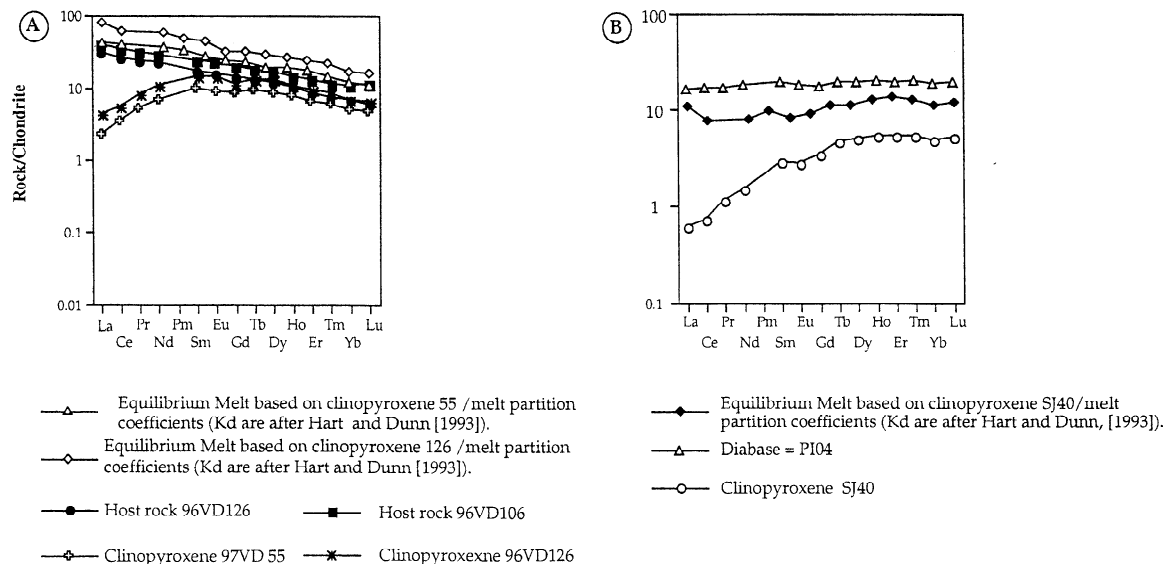
Figure 9. Rare earth$_N$ patterns of calculated melts in equilibrium with the Duarte (Dominican Republic) and Piñón (Ecuador) clinopyroxenes. Chondrite values are from Sun and McDonough [1989].

Their Th/U ratios are low. The Duarte cpx is less LREE depleted than that of Ecuador and is in equilibrium with a cpx-rich basaltic melt, similar to 96VD106. The cpx from Ecuador is in equilibrium with an enriched tholeiitic melt. The Arperos basalts exhibit intermediate geochemical features between those of the Duarte and Piñón rocks.

6. Isotopic Chemistry of the Mineral Separates and Host Rocks

6.1. The cpx-Rich Basalts of the Duarte Complex

As already mentioned, all data were corrected for in situ decay assuming an age of 86 Ma for this formation. The 96VD126 cpx and its cumulate-enriched cpx-rich host rock have similar ε_{Nd} ratios (+8.34 and 8.53, respectively; Table 3 and Figure 10) while that of the amphibole is slightly lower (7.99). In contrast, the $(^{87}Sr/^{86}Sr)_i$ of the amphibole and its host rock are exactly the same (0.70315; Table 3) and plot in the same range as the associated cpx (0.70320). The cpx-rich basalt, cumulus-enriched rocks (97VD55, 96VD121) and their constituent cpx have rather homogeneous ε_{Nd} (+7.6 < ε_{Nd} < 6.2; Table 3) which are significantly lower than those of the 96VD126 rock and constituent minerals. The cpx of the cpx-rich basalt (96VD106) differs from the previous rocks by having a slightly lower ε_{Nd} ratio (+5.5; Table 3 and Figure

10), although its host rock displays ε_{Nd} (+6.4) in the same range as other sampled rocks of this complex.

Similarly, the initial Sr isotopic ratio of the 96VD106 cpx is slightly higher (0.70362; Table 3) than that of the corresponding whole rock (0.70370; Table 3). We attribute this difference to the presence of actinolite which locally rims the cpx. These Mg-rich rocks and their minerals (with the exception of the cumulus-enriched 96VD121) have homogeneous $(^{87}Sr/^{86}Sr)_i$ (0.70315 < $(^{87}Sr/^{86}Sr)_i$ < 0.70370; Table 3 and Figure 10), which probably reflects their source composition.

Initial lead isotopic compositions of whole rocks and mineral separates from Mg-rich basalts of the Duarte Complex display a limited range of $^{206}Pb/^{204}Pb$ (18.97-19.54), $^{207}Pb/^{204}Pb$ (15.52-15.60), and $^{208}Pb/^{204}Pb$ (38.6-39.3) (Table 3 and Figure 11). These highly radiogenic isotopic compositions fall within the range of enriched OIB signatures. Interestingly, the Duarte Complex domain falls close to or on the Northern Hemisphere Reference Line (NHRL [Zindler and Hart, 1986]) in the $^{207}Pb/^{204}Pb$-$^{206}Pb/^{204}Pb$ isotope diagram but on or slightly above the NHRL in the $^{208}Pb/^{204}Pb$-$^{206}Pb/^{204}Pb$ isotope diagram.

6.2. Basalts, Diabases, and Cumulate Gabbro From Ecuador and Mexico

In an attempt to obtain a reliable constraint on the age of the Piñón suite, we determined a Sm/Nd internal isochron on

DUARTE
- ■ Cpx, amphibole and host rock 96VD126
- ▲ Cpx and host rock 97VD55
- ▼ Whole rock 96VD121
- ✦ Cpx and host rock 96VD106

ECUADOR
- ◇ Diabases (EQ1, EQ12, CA1)
- □ Cpx and host rock diabase PIO4
- ○ Cpx and hornblende SJ40

WESTERN MEXICO | ✳ Arperos basalts

✧ Cretaceous basalts and picrites [Kerr et al., 1996a, b]
+ Cretaceous Colombian basalts and intrusives [Kerr et al., 1997a]
● Dumisseau basalts from Haiti [Sen et al., 1988]
▨ Gorgona komatiites
▤ Gorgona depleted basalts
▧ Gorgona enriched basalts
▢ Galápagos
▦ Ontong Java and Nauru

Figure 10. The ε_{Nd} -ε_{Sr} and ε_{Nd} -$(^{87}Sr/^{86}Sr)_i$ plots for the minerals and host rocks from Dominican Republic, Ecuador, and westerncentral Mexico.
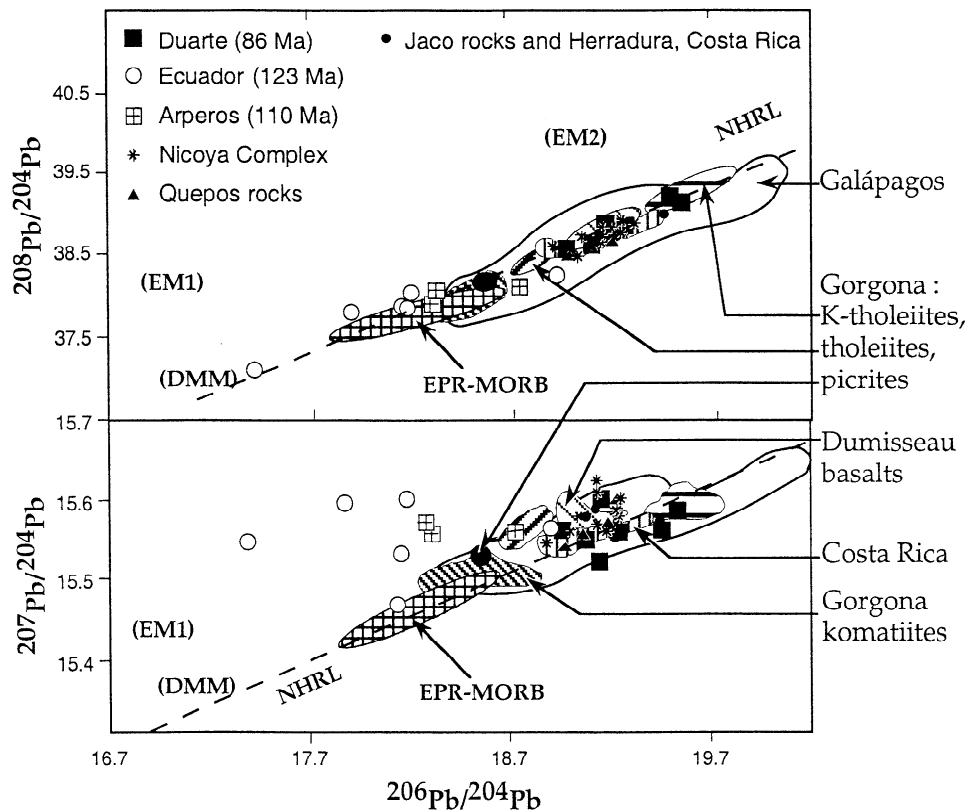
Figure 11. The ^{208}Pb-^{204}Pb versus ^{206}Pb-^{204}Pb and ^{207}Pb-^{204}Pb versus ^{206}Pb-^{204}Pb correlation diagrams for the minerals and host rocks. Recalculated initial ratios have been reported for minerals and whole rocks from cumulates and clinopyroxene-rich basalts from Dominican Republic (86 Ma), gabbros and diabases from Ecuador (123 Ma), and pillow basalts from Arperos from Mexico (110 Ma). Typical analytical uncertainties are indicated by the size of the symbols. Various analytical points and data fields have been reported from the literature. Data from the Nicoya Complex, Jaco rocks and Herradura, Costa Rica (90 Ma), are after *Hauff et al.* [1997], and *Sinton et al.* [1997 and 1998]. The Gorgona picrites, komatiites; tholeiites; and K-tholeiites fields are after *Dupré and Echeverria* [1984]. The field of the Dumisseau basalts from Haiti field is from *Sen et al.* [1988]. The Galápagos lavas field is reported by *White et al.* [1993]. East Pacific MORB data and Galapagos Islands field are from *White et al.* [1987, 1993].

the SJ13 amphibole gabbro (Table 4). The three experimental points (whole rock, plagioclase, and amphibole) yield a regression age of 123±13 Ma with a ^{143}Nd/^{144}Nd initial ratio of 0.512875±37 (mean square of weighted deviation, MSWD = 2.05) [*Ludwig*, 1987] (Figure 12). This age is interpreted as corresponding to the crystallization of the cumulate gabbro in the oceanic plateau section, now exposed in Ecuador. It also indicates that plateau-building eruptions occurred in the Ecuadorian province as early as 123 Ma. Meanwhile, the rather large uncertainty of this age needs to be refined by additional analyses.

In common with the minerals and host rocks of the Duarte Complex the diabases, basalts, gabbro, and associated cpx from Ecuador and Mexico share rather similar homogeneous ε_{Nd} ratios that range between +8 and +5.8 (Table 3) (Reynaud *et al.*, submitted manuscript, 1998). The SJ40 plagioclase has a slightly lower ε_{Nd} (+4.62, Table 3). However, a diabase (EQ1) and a basalt (CA1) from Ecuador have higher (ε_{Nd} = +10) and lower ε_{Nd} (+4.5) ratios, respectively (Table 3 and Figure 10). This suggests that the basalts and diabases from Ecuador and Mexico might be derived from different mantle sources and/or different blends of depleted NMORB and enriched OIB magma types.

In the ε_{Nd} versus ε_{Sr} diagram (Figure 10), all these rocks fall within the "mantle array," and their (^{87}Sr/^{86}Sr)$_i$ likely reflects the source composition, with the exception of three basalts from western Mexico (M92-64, M93-17, and CA1). The shift of the Sr isotopic ratios of these three rocks toward the radiogenic side of the mantle plot reflects an enrichment in radiogenic Sr (Figure 10), probably induced by seawater contamination through hydrothermal process or contamination with pelagic sediment [*Kerr et al.*, 1997b].

Lead initial isotopic compositions of whole-rocks and mineral separates from basalts and cumulate gabbros from Ecuador and Mexico have a large range of ^{206}Pb/^{204}Pb and ^{208}Pb/^{204}Pb ratios (Table 3 and Figure 11). Diabase EQ12 has a markedly lower ^{206}Pb/^{204}Pb ratio and plots near the depleted mantle MORB (DMM) source. In constrast, CA1 has a significantly higher ^{206}Pb/^{204}Pb ratio similar to those of recent Galápagos lavas. The Ecuador samples define a nearly horizontal domain located slightly above the NHRL in the ^{207}Pb/^{204}Pb diagram. These high ^{207}Pb/^{204}Pb ratios could reflect a contamination of their mantle sources by pelagic sediments [*Doe*, 1970] and/or altered oceanic crust.

In summary, all samples from Dominican Republic, Ecuador, and western Mexico have fairly homogeneous ε_{Nd}
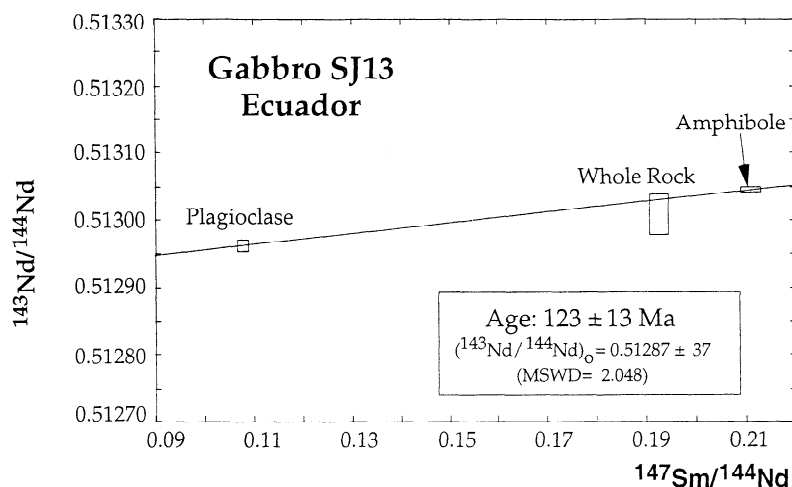
Figure 12. Sm/Nd isochron plot for minerals and whole-rock from the Ecuadorian SJ13 Gabbro. The regression analysis [Ludwig, 1987] yields T = 123 ± 13 Ma, $(^{143}Nd/^{144}Nd)_0$ = 0.512875 ± 37, εNd_0 = +7.76, and MSWD = 2.05 for plagioclase, whole rock and Amphibole.

(+5.5 to +8), similar to those of oceanic plateau basalts. The cpx of the Duarte cumulus-enriched basalt has slightly higher εNd (+8.5). Finally, one mafic rock of the Piñón Formation has the highest εNd (+10), similar to those of NMORB. A comparison of initial Pb isotopic signatures measured (on mineral separates and host rocks) on cumulus-enriched Mg-rich basalts from the Duarte Complex, on gabbros and diabases from Ecuador, and on Arperos basalts from Mexico emphasize a contribution from a more depleted mantle source for Ecuador than for the Duarte Complex. Mg-rich basalts from the Dominican Republic (Duarte) have a Pb isotopic range consistent with that of the Galápagos HIMU plume component and similar to the Gorgona tholeiites and Costa Rican lavas [White et al., 1993; Dupré and Echeverria, 1984; Hauff et al., 1997; Sinton et al., 1997]. The Ecuadorian and Mexican basalts and cumulate gabbros have a Pb isotopic signature intermediate between NMORB and OIB components.

7. Discussion: Presence of Three Distinct Magmatic Suites in the CCOP

A major difficulty in constraining the geochemical and isotopic characteristics of oceanic plateau igneous rocks arises from the low grade metamorphism or hydrothermal alteration that these rocks suffered either during their magmatic emplacement and cooling in a submarine environment and/or during their subsequent tectonic emplacement. These processes resulted in the mobility of Rb, Sr, and U, as suggested by the variable behavior observed for these elements in most spidergrams (Figure 6), despite the fact that in this study we have deliberately chosen to focus our geochemical and isotopic investigations on a restricted number of samples and host minerals showing minimum alteration. However, the observation that most whole rock REE patterns fit with those calculated from the compositions of separated primary cpx indicates that the REE distribution was not significantly affected by postmagmatic processes. In addition, the analysis of separates of unaltered primary minerals allows us to check that the corresponding bulk rock compositions did not suffer

noticeable Nd and Pb (and, in most cases, Sr) isotopic changes related to hydrothermal alteration (i.e., 96VD126 and SJ40, Table 3).

On the basis of ages, rock types, and geochemical and isotopic results the ultramafic-mafic oceanic crustal fragments currently regarded as belonging to the CCOP appear to belong to three distinct magmatic suites. The Upper Cretaceous suite (92-86 Ma) comprising the Gorgona basalts is the best known and geochemically well characterized. It makes up the basement of the Caribbean Sea and part of the numerous accreted oceanic crustal fragments exposed along the Pacific coast of Central America (Costa Rica) and South America (Colombia) and in the Caribbean (Dominican Republic, most of Duarte Complex; Curaçao, and Aruba; Figure 1). The basalts and diabases have LREE-enriched to flat REE patterns and differ from NMORB by their enrichments in Ti, Nb, Th, and Ta. Initial radiogenic Nd isotope ratios have a rather restricted compositional range (εNd = +6 to +9.5 [Sen et al., 1988; Kerr et al., 1996b, 1997b; Alvarado et al., 1997; Hauff et al., 1997; Sinton et al., 1997]). Similarly, all these rocks have a Pb isotopic signature consistent with the field defined by the recent Galápagos Islands, suggesting the contribution of a HIMU component (Figure 11).

The age of the second suite, composed of the Ecuadorian and Mexican oceanic rocks, is Early Cretaceous (123-91 Ma). The corresponding rocks have a wide range of initial radiogenic Nd and Pb isotopic ratios, intermediate between OIB and NMORB components. The Ecuadorian igneous rocks, compared to those of the Dominican Late Cretaceous Duarte Complex, are depleted in the most incompatible elements.

Finally, in the Duarte and Nicoya Complexes (Figure 1), slices of Upper Jurassic oceanic rocks are tectonically associated with the Upper Cretaceous oceanic plateau tholeiites. Indeed, these Upper Jurassic basalts and diabases from Dominican Republic differ from the Duarte cpx-enriched and/or cpx-poor basalts because they are depleted in LREE and in most incompatible trace elements [Lapierre et al., 1999]. Thus these basalts and diabases are interpreted as remnants of the Late Jurassic Caribbean oceanic crust formed at a ridge and possibly close to a hospot.

In Costa Rica, Upper Jurassic radiolarian cherts were probably deposited on the top of oceanic crust [*Sinton et al.,* 1997]. In Hispaniola, slices of Upper Jurassic oceanic crust are tectonically associated with the Late Cretaceous Duarte Complex (see section 6).

In summary, at least two major pulses of oceanic plateau magmas occurred in the CCOP: Late Cretaceous (88-92 Ma) and Early Cretaceous (100-123 Ma). The Late Cretaceous cpx-rich basalts share the HIMU affinity of the Galápagos hotspot, while those of the Early Cretaceous plutonic and volcanic rocks are intermediate between depleted and HIMU mantle sources.

8. Geodynamic Implications

The presence of two distinct oceanic plateau suites in the crustal fragments of the peri-Caribbean realm raises two questions.

1. Are these suites derived from two distinct hotspots possessing different signatures, as suggested by *Kerr et al.* [1997a], or solely from the Galápagos one?

2. If they are both derived from the Galápagos hotspot, is the present-day geographic location of the Ecuadorian and Mexican Early Cretaceous oceanic terranes consistent with the locations of the Galápagos plume and South America and the direction of Farallon plate motion during the Early Cretaceous, respectively?

If both suites are linked to the Galápagos plume this implies that (1) the activity of the Galápagos plume began at least in Early Cretaceous times (or even before); (2) its isotopic composition has changed markedly with time from low to high $^{206}Pb/^{204}Pb$ values; (3) it was heterogenous and different parts were tapped in different places; and (4) its location was possibly close to or on a ridge, similar to that of the Iceland plume; [*Kerr et al.,* 1995]. It has been proposed that many of the Pacific plateaus (i.e., Shatsky, Ontong Java, Manihiki) may have been formed above long-lived, near-mid-ocean ridge or ridge-centered Cretaceous hotspots (140-65 Ma) [*Mahoney,* 1987]. Moreover, the Pb isotopic composition of the hotspot may change with time, i.e., the source of the Ontong Java plateau lavas shows an evolution with time from lower to higher $^{206}Pb/^{204}Pb$ ratio [*Mahoney et al.,* 1993].

The Ecuadorian and Mexican igneous terranes (1) could reflect an early stage of the Galápagos hotspot activity which would have lasted from 123 Ma to 86 Ma, or (2) could have formed from a possible precursor which would have been only active during a short time at the early Cretaceous or alternatively could have formed somewhere other than at the Galápagos hotspot.

Some plate tectonic constraints are important in this discussion. For example, the development of a magmatic arc through Ecuador and Colombia during the Jurassic suggests that the Farallón plate was subducting southeastward under the northwestern margin of South America [*Aspden et al.,* 1987; *Jaillard et al.,* 1995]. However, during the latest Jurassic (≈ 140-135 Ma) the activity of the continental magmatic arc stopped in Ecuador and Colombia and a new magmatic arc developed along the Peruvian margin [*Aspden et al.,* 1987; *Jaillard et al.,* 1995]. This feature suggests that the subducting motion of the Farallón Plate beneath South America drastically changed toward a NNE motion during the latest Jurassic, and

this motion persisted until Late Cretaceous times (≈ 80 Ma) [*Jaillard et al.,* 1995]. If the Ecuadorian Early Cretaceous oceanic or older plateau fragments had been derived from the Galápagos hotspot, they should be presently located far NNE from the present-day Galápagos Islands. Therefore they are more probably linked to an another hotspot, which was located much farther southwest of the South American plate than the Galápagos. In contrast, the Early Cretaceous accreted oceanic plateau fragments from western Mexico could have formed at the Galápagos hotspot.

The Late Cretaceous (92-86 Ma) crustal oceanic fragments exposed presently in Costa Rica (Nicoya Peninsula), in the Caribbean region (Dominican Republic, Curaçao, Aruba), and in the Western Cordillera of Colombia are characterized by a rather large range of ε_{Nd} ratios (+9 to +6) and a limited range of lead isotopic compositions that fall within the field of the recent Galápagos Islands. This suggests that the Late Cretaceous (92-86 Ma) oceanic fragments were most probably linked to the igneous activity of the Galápagos plume, whereas the hospot from which the oldest fragments were derived remains unknown. More data are needed to geochemically characterize the fragments of the CCOP and to understand its chronological and geodynamic development.

9. Conclusions

The oceanic plateau fragments of the CCOP exposed in central Mexico, Dominican Republic, and coastal Ecuador belong to two distinct suites which differ in their age and trace element and isotopic chemistry.

1. The minerals and cumulus-enriched host rocks of the Duarte Complex (Dominican Republic), dated at 86 ± 1.4 Ma, have LREE-enriched patterns; moderate enrichments in large ion lithophile elements (LILE); high Nb, Ta, and Pb contents; homogeneous ε_{Nd} ratios (+8 to +5) and radiogenic Pb isotopic compositions, very similar to the Galápagos HIMU component. They are geochemically similar to the Late Cretaceous mafic and ultramafic rocks (with the exception of the Gorgona komatiites, picrites from SW Colombia [*Kerr et al.,* 1997a]) of the CCOP and likely derived from the Galápagos hotspot.

2. The Early Cretaceous (> 91 Ma) diabases and basalts (Piñón Formation) and cumulate gabbros (123 Ma) from western Ecuador differ from the Duarte Mg-rich rocks by flat REE patterns and lower Pb, Zr, Hf, Th, and U contents. The Lower Cretaceous basalts and diabases from Mexico (Arperos Formation) exhibit intermediate trace element compositions between the Duarte and Piñón rocks. Both Ecuadorian and Mexican rocks have also a wider range of ε_{Nd} and Pb isotopic ratios that range between those of NMORB or depleted plume and HIMU sources. Geochemical constraints alone are not really conclusive because there is ample evidence for geochemical variability of magmas originating from a single plume but derived from variable melting degrees of heterogeneous sources [*Arndt et al.,* 1996; *Kerr et al.,* 1996a]. These geochemical features of the Ecuadorian and Mexican mafic rocks suggest that they derived from a ridge-centered, or near ridge hotspot.

The Caribbean-Colombian plateau was likely formed during two major pulses of Late Cretaceous and Early Cretaceous, respectively. The Late Cretaceous pulse is likely linked to the

Galápagos hotspot whereas that of Early Cretaceous probably derived from a near-ridge hotspot, located farther SW of South America, somewhere in the SE Pacific.

References

Aitken, B. G., and L. M. Echeverria, Petrology and geochemistry of komatiites and tholeiites from Gorgona Island, Colombia, *Contrib. Mineral. Petrol, 86,* 94-105, 1984.

Alvarado, G. E., P. Denyer, and C. W. Sinton, The 89 Ma Tortugal komatiitic suite, Costa Rica: Implications for a common geological origin in the Caribbean and eastern Pacific region from a mantle plume, *Geology, 25,* 439-442, 1997.

Arndt, N. T., A. C. Kerr, and J. Tarney, Differentiation in plume heads: The formation of Gorgona komatiites and basalts, *Earth Planet. Sci. Lett., 146,* 289-301, 1996.

Aspden, J. A., and M. Litherland, The geology and Mesozoic collisional history of the Cordillera Real, Ecuador, *Tectonophysics, 205,* 187-204, 1992.

Aspden, J. A., W. J. McCourt, and M. Brook, Geometrical control of subduction-related magmatism: The Mesozoic and Cenozoic plutonic history of Western Colombia, *J. Geol. Soc. London, 144,* 893-905, 1987.

Aspden, J. A., S. H. Harrison, and C. C. Rundle, New geochronological control for the tectono-magmatic evolution of the metamorphic basement, Cordillera Real and El Oro Province of Ecuador, *J. S. Am. Earth Sci., 6,* 77-96, 1992.

Barrat, J.-A., F. Keller, J. Amossé, R. N. Taylor, R.W. Nesbitt, and T. Hirata, Determination of rare earth elements in sixteen silicate reference samples by ICP-MS using a Tm addition and an ion-exchange chromatography procedure, *Geostand. Newsl. XX,* 133-139, 1996.

Ben-Avraham, Z. A., A. Nur, D. Jones, and A. Cox, Continental accretion: from oceanic plateaus to allochthonous terranes, *Science, 213,* 47-54, 1981.

Bourgois, J., A. Egüez, J. Butterlin, and P. de Wever, Evolution géodynamique de la Cordillère Occidentale des Andes d'Equateur: La découverte de la formation éocène d'Apagua, *C. R. Acad. Sci. Ser. II, 311,* 173-180, 1990.

Bowin, C., Geology of the Central Dominican Republic (case history part of an island arc), in *Caribbean Geological Studies,* edited by H. H. Hess, *Geol. Soc. Am. Mem., 98,* 11-84, 1966.

Bowin, C. O., The geology of Hispaniola, in *The Ocean Basins and Margins,* vol. 3, *The Gulf of Mexico and the Caribbean,* edited by A. E. M Nairn and F. G. Stehli, pp. 501-552, Plenum, New York, 1975.

Burke, K., P. Fox, and A. M. C. Sengör, Buoyant ocean floor and the evolution of the Caribbean, *J. Geophys. Res., 83,* 3949-3954, 1978.

Cloos, M., Lithospheric buoyancy and collisional orogenesis: Subduction of oceanic plateaus, continental margins, island arcs, spreading ridges, and seamounts, *Geol. Soc. Am. Bull., 105,* 715-737, 1993.

Cosma L., H. Lapierre, É. Jaillard, G. Laubacher, D. Bosch, A. Desmet, M. Mamberti, and P. Gabriele, Pétrographie et géochimie des unités de la Cordillère Occidentale d'Équateur (0°30's): implications tectoniques, *Bull. Soc. Géol. Fr., 169,* 739-751, 1998.

Dávila Alcocer A.V.M., and J. Martínez Reyes, Una edad cretácica para las rocas basales de la Sierra de Guanajuato, paper presented at Simposio sobre la Geología de la Sierra de Guanajuato, Inst. Geol., Univ. Nac. Auto. de México, 1987.

Desmet, A., Ophiolites et séries basaltiques crétacées des régions caraïbes et nord-andines: bassins marginaux, dorsales ou plateaux océaniques?, Doctorat d'état thesis, 589 pp., Univ. Nancy 1, Nancy, France, 1994.

Doe, B. R., *Lead Isotopes,* 137 pp., Springer- Verlag, New York, 1970.

Donnelly, T. W., W. Melson, R. Kay, and J.J.W. Rogers, Basalts and dolerites of late Cretaceous age from the central Caribbean, *Initial Rep. Deep Sea Drill. Proj., 15,* 989-1012, 1973.

Donnelly, T. W., et al., History and tectonic setting of Caribbean magmatism, in *The Geology of North America,* vol. H, *The Caribbean Region,* edited by G. Dengo and J.E. Case, pp. 339-374, Geol. Soc. of Am., Boulder, Colo., 1990.

Draper, G., and J. F. Lewis, Metamorphic belts in central Hispaniola, in *Geologic and Tectonic Development of the North America-Caribbean Plateau Boundary in Hispaniola,* edited by P. Mann, G. Draper, and J. F. Lewis, *Geol. Soc. Am. Spec. Pap. 262,* 29-45, 1991.

Duncan, R.A., and R. B. Hargraves, Plate tectonic evolution of the Caribbean region in the mantle reference frame, in *The Caribbean-South American Plate Boundary and Regional Tectonics,* edited by W. E. Bonini et al., *Mem. Geol. Soc. Am., 162,* 81-94, 1984.

Dupré, B., and L. M. Echeverria, Pb isotopes of Gorgona island (Colombia): Isotope variations correlated with magma type, *Earth Planet. Sci. Lett., 67,* 186-190, 1984.

Dupuis, V., H. Lapierre, B. Mercier de Lépinay, R. C. Maury, M. Tardy, and J. Hernandez, The Duarte complex (Hispaniola) revisited: Evidence for three structural units in a remnant of the Caribbean oceanic plateau, *Terra Nova, 9,* 525, 1997.

Freydier, C., J. Martínez R., H. Lapierre, M. Tardy, and C. Coulon, The Early Cretaceous Arperos oceanic basin (western Mexico): Geochemical evidence for an aseismic ridge formed near a spreading center. *Tectonophysics, 259,* 343-367, 1996.

Goossens, P. J., and W. I. Rose, Chemical composition and age determination of tholeiitic rocks in the basic Cretaceous Complex, Ecuador, *Geol. Soc. Am. Bull., 84,* 1043-1052, 1973.

Gradstein, F. M., F. P. Agterberg, J. G. Ogg, J. Hardenbol, P. van Veen, J. Thierry, and Z. Huang, A Mesozoic time scale, *J. Geophys. Res. 99,* 24,051-24,074, 1994.

Hart, S. T., and T. Dunn, Experimental cpx/melt partitioning of 24 trace elements, *Contrib. Mineral. Petrol., 113,* 1-8, 1993.

Hauff, F., K. Hoernle, H.-U. Schminke, and R.A. Werner, Mid-Cretaceous origin for the Galápagos Hotspot: Volcanological, petrological and geochemical evidence from Costa Rican oceanic crustal fragments, *Geol. Rundsch.*, 86, 141-155, 1997.

Jaillard, É., T. Sempéré, P. Soler, G. Carlier, and R. Marocco, The role of Tethys in the evolution of the Northern Andes between Late Permian and Late Eocene times, in edited by A.E.M. Nairn, L.-E. Ricou, B. Vrielynk, and J. Dercourt, *Ocean Basins and Margins, vol. 8, The Tethys Ocean*, pp. 463-492, Plenum, New York, 1995.

Jaillard, É., M. Ordoñez, P. Bengtson, G. Berrones, M. Bonhomme, N. Jiménez, and I. Zambrano, Sedimentary and tectonic evolution of the arc zone of southwestern Ecuador during Late Cretaceous and Early Tertiary times, *J. S. Am. Earth Sci.*, 9, 131-140, 1996.

Juteau, T., F. Mégard, L. Raharison, and H. Whitechurch, Les assemblages ophiolitiques de l'Occident équatorien: Nature pétrographique et position structurale, *Bull. Soc. Géol. Fr.*, 19, 1127-1132, 1977.

Kerr, A. C., A. D., Saunders, J. Tarney, N. H. Berry, and V. L. Hards, Depleted mantle plume geochemical signatures: No paradox for plume theories, *Geology*, 23, 843-846, 1995.

Kerr, A. C., G. F., Marriner, N. T. Arndt, J. Tarney, A. Nivia, A. D. Saunders, and R. A. Duncan, The petrogenesis of Gorgona komatiites, picrites and basalts: New field, petrographic and geochemical constraints, *Lithos*, 37, 245-260, 1996a.

Kerr, A. C., J. Tarney, G. F. Marriner, A. Nivia, and A.D. Saunders, The geochemitry and tectonic setting of Late Cretaceous Caribbean and Colombian volcanism, *J. S. Am. Earth Sci.*, 9, 111-1201, 1996b.

Kerr, A. C., J. Tarney, G. F. Marriner, G. T. Klaver, A. D. Saunders, and M. F. Thirwall, M. F., The geochemistry and petrogenesis of the late Cretaceous picrites and basalts from Curaçao, Netherlands Antilles: A remnant of an oceanic plateau, *Contrib. Mineral. Petrol.*, 124, 29-43, 1996c.

Kerr, A. C., G. F. Marriner, J. Tarney, J., A. Nivia, A. D. Saunders, M. F. Thirlwall, and C. W. Sinton, Elemental and Isotopic constraints on the petrogenesis and origin of Cretaceous basaltic terranes in western Colombia, *J. Petrol.*, 38, 677-702, 1997a.

Kerr, A. C., J. Tarney, G. F. Marriner, A. Nivia, and A. D. Saunders, The Caribbean-Colombian Cretaceous Igneous Province: The internal anatomy of an Oceanic Plateau, in *Large Igneous Provinces, Continental, Oceanic and Planetary Flood Volcanism, Geophys. Monogr. Ser.*, vol. 100, edited by M. F. Coffin and J. J. Mahoney, pp. 123-144, AGU, Washington, D. C., 1997b.

Kesler, S. E., J. F. Lewis, L. M. Jones, and R. L. Walker, R. L., Early island arc intrusive activity, Cordillera Central, Dominican Republic, *Contrib. Mineral. Petrol.*, 65, 91-99, 1977.

Lapierre, H., V. Dupuis, B. Mercier de Lépinay, M. Tardy, J. Ruiz, R. C. Maury, J. Hernandez, and M. Loubet, Is the Lower Duarte Igneous Complex (Hispaniola) a remnant of the Caribbean plume generated oceanic plateau?, *J. Geol.*, 105, 111-120, 1997.

Lapierre, H., *et al.*, Late Jurassic oceanic crust and Upper Cretaceous Caribbean Plateau picritic basalts exposed in the Duarte Igneous Complex, *J. Geol.*, in press, 1999.

Lavenu, A., G. Noblet, M. Bonhomme, A. Egüez, F. Dugas, and G. Vivier, New K-Ar age dates of Neogene and Quaternary volcanic rocks from the Ecuadorian Andes: Implications for the relationship between sedimentation, volcanism and tectonics, *J. S. Am. Earth Sci.*, 5, 309-320, 1992.

Lebrat, M., F. Mégard, C. Dupuy, and J. Dostal, Geochemistry and tectonic setting of pre-collision Cretaceous and Paleogene volcanic rocks of Ecuador, *Geol. Soc. Am. Bull.*, 99, 569-578, 1987.

Lewis, J. F., and J. G. Jiménez, The Duarte Complex in the La Vega-Jarabacoa-Janico area, central Hispaniola: Geologic and geochemical features of the sea floor during the early stages of arc evolution, in *Geologic and Tectonic Development of the North America-Caribbean Plateau Boundary in Hispaniola*, edited by P. Mann, G. Draper, and J. F. Lewis, *Spec. Pap. Geol. Soc. Am.*, 262, 115-141, 1991.

Ludwig, K. R., Isoplot 200, a plotting and regression program for isotope geochemists, for use with HP series 200 computers, *U. S. Geol. Surv.* Open-file report, 85-513, 1987.

Mahoney, J. J., An isotopic survey of Pacific oceanic plateaus: implication for their nature and origin, in *Seamounts, Islands, and Atolls, Geophys. Monogr. Ser.* vol. 43, edited by B. Keating, P. Fryer, R. Batiza, and G. Boehlert, pp. 207-220, AGU, Washington D. C., 1987.

Mahoney, J. J., M. Storey, R.A. Duncan, K.J. Spencer, and M. Pringle, Geochmistry and Age of the Ontong Java Plateau, in *The Mesozoic Pacific: Geology, Tectonics and Volcanism, Geophys. Monogr. Ser.*, vol. 77, edited by M. S. Pringle, W. S. Sager, W. V. Sliter, and S. Stein, pp. 233-261, AGU, Washington, D. C., 1993.

Manhès, G., C. J. Allègre, B. Dupré, and B. Hamelin, Lead isotope study of basic-ultrabasic layered complex: speculations about the ages of the Earth and primitive mantle characteristics, *Earth Planet. Sci. Lett.*, 43, 370-382, 1980.

Mercier de Lépinay, B., L'évolution géologique de la bordure nord-caraïbe: L'exemple de la transversale de l'île d'Hispaniola (Grandes Antilles), thèse d'état, *Univ. Pierre et Marie Curie*, 336 pp, Paris, 1987.

Montgomery, H., E. A. Pessagno, J. F. Lewis, and J. Schellekens, Paleogeography of Jurassic fragments in the Caribbean, *Tectonics*, 13, 725-732, 1994.

Noble, S. R., J. A. Aspden, and R. Jemielita, Northern Andean crustal evolution: New U-Pb geochronological constraints from Ecuador, *Geol. Soc. Am. Bull.*, 109, 789-798, 1997.

Nur, A., and Z. Ben-Avraham, Oceanic plateaus, the fragmentation of continents, and mountain building, *J. Geophys. Res.*, 87, 3644-3661, 1982.

Palmer H., Geology of the Moncion-Jarabacoa area, Dominican Republic, Hispaniola, in *Tectonic Focal Point of the Northern Caribbean*, edited by B. Lidz, and F. Nagle, pp. 29-68, Miami Geol. Soc., Miami, Fla., 1979.

Saunders, A. D., J. Tarney, A. C. Kerr, and R. W. Kent, The formation and fate of of large igneous provinces, *Lithos*, 37, 81-95, 1996

Sen, G., R. Hickey-Vargas, D. G. Waggoner, and F. Maurrasse, Geochemistry of basalts from the Dumisseau Formation, southern Haiti: Implications for the origin of the Caribbean sea crust, *Earth Planet. Sci. Lett.*, 87, 423-437, 1988.

Sigurdsson, H., et al., Caribbean ocean history and the Cretaceous-Tertiary boundary event, *Proc. Ocean Drill. Program Initial Rep.*, 165, 377-400, 1997.

Sinton, C. W., R. A. Duncan, and P. Denyer, Nicoya Peninsula, Costa Rica, A single suite of Caribbean oceanic plateau magmas, *J. Geophys. Res., 102,* 15,507-15,520, 1997.

Sinton, C. W., M. Storey, J. Lewis, and J. J. Estrada, An oceanic flood basalt within the Caribbean plate, *Earth Planet. Sci. Lett., 155,* 221-235, 1998.

Sun, S. S., and W. F. McDonough, Chemical and isotopic systematics of oceanic basalts: Implications for mantle composition and processes, in *Magmatism in Ocean Basins,* edited by A. D. Saunders and M. J. Norry, *Geol. Soc. Spec. Publ., London, 42,* 279-292, 1989.

Tardy, M., J.-C. Carfantan, and C. Rangin, Essai de synthèse sur la structure du Mexique, *Bull. Soc. Géol. Fr., Ser. II, 6,* 1025-1031, 1986.

Tejada, M. L. G., J. J. Mahoney, R. A. Duncan, and M. P. Hawkins, Age and geochemistry of basement and alkalic rocks of Malaita and Santa Isabel, Solomon Islands, and southern margin of the Ontong Java Plateau, *J. Petrol., 37,* 361-394, 1996.

Toussaint, J.-F., and J. J. Restrepo, The Colombian Andes during Cretaceous times, in *Cretaceous Tectonics in the Andes,* edited by J. A. Salfity, pp. 61-100, F. Viewcg, Braunschweig, Germany, 1994.

White, W. M., and R. A. Duncan, Geochemistry and geochronology of the Society Islands: New evidence for deep mantle recycling, in *Earth Processes: Reading the Isotopic Code, Geophys. Monogr. Ser.,* vol. 95, edited by A. Basu and S. R. Hart, pp. 183-206, AGU, Washington, D.C., 1996.

White, W. M., A.W. Hofmann, and H. Puchelt, Isotope geochemistry of Pacific mid-ocean ridge basalt, *J. Geophys. Res., 92,* 4881-4893, 1987.

White, W. M., A. R. McBirney, and R. A. Duncan, Petrology and geochemistry of the Galápagos Islands: Portrait of a pathological mantle plume, *J. Geophys. Res., 98,* 19,533-19,563, 1993.

Zindler, A., and S. Hart, Chemical geodynamics, *Annu. Rev. Earth Planet. Sci., 14,* 493-571, 1986.

D. Bosch and P. Monié, UMR 5567-CNRS, Université Montpellier II, Place Eugène Bataillon, 34095 Montpellier, France. (bosch@dstu.univ-montp2.fr)

A. Desmet, Laboratoire de Pétrologie, Université Henri Poincaré, B.P. 239, 54506 Vandoeuvre lés Nancy, France.

V. Dupuis and B. Mercier de Lépinay, UMR-6526 CNRS, Université de Nice Sophia-Antipolis, rue Albert Einstein, 06500 Valbonne, France. (dupuis@faille.unice.fr)

J. Hernandez, Institut de Minéralogie, Université de Lausanne, BSFH 2, 1015 Lausanne, Switzerland. (Jean.Hernandez@imp.unil.ch)

E. Jaillard, F. Keller, H. Lapierre, M. Mamberti, and F. Sénebier, UPRESA 5025 CNRS, Université Joseph Fourier, 15 rue M. Gignoux, 38031 Grenoble, France. (ejaillard@ujf-grenoble.fr, lapierre@ujf-grenoble.fr,)

R. C. Maury, UMR 6538-CNRS, Université de Bretagne occidentale, B. P. 809, 29285 Brest Cédex, France. (maury@cassis-gw.univ-brest.fr)

M. Polvé and D. Yeghicheyan, UMR 5563-CNRS, Université Paul Sabatier, 38 rue des 36-Ponts, 31400 Toulouse, France. (polve@lucid.ups-tlse.fr)

M. Tardy, UPRESA 5025 CNRS, Université de Savoie, B.P. 1104, 73011 Chambéry, France. (tardy@univ-savoie.fr)